Probability distributions of molecular observables computed from Markov models

Frank Noé[a)]
DFG Research Center Matheon, FU Berlin, Arnimallee 6, 14159 Berlin, Germany

(Received 23 January 2008; accepted 3 April 2008; published online 23 June 2008)

Molecular dynamics (MD) simulations can be used to estimate transition rates between conformational substates of the simulated molecule. Such an estimation is associated with statistical uncertainty, which depends on the number of observed transitions. In turn, it induces uncertainties in any property computed from the simulation, such as free energy differences or the time scales involved in the system's kinetics. Assessing these uncertainties is essential for testing the reliability of a given observation and also to plan further simulations in such a way that the most serious uncertainties will be reduced with minimal effort. Here, a rigorous statistical method is proposed to approximate the complete statistical distribution of any observable of an MD simulation provided that one can identify conformational substates such that the transition process between them may be modeled with a memoryless jump process, i.e., Markov or Master equation dynamics. The method is based on sampling the statistical distribution of Markov transition matrices that is induced by the observed transition events. It allows physically meaningful constraints to be included, such as sampling only matrices that fulfill detailed balance, or matrices that produce a predefined equilibrium distribution of states. The method is illustrated on μs MD simulations of a hexapeptide for which the distributions and uncertainties of the free energy differences between conformations, the transition matrix elements, and the transition matrix eigenvalues are estimated. It is found that both constraints, detailed balance and predefined equilibrium distribution, can significantly reduce the uncertainty of some observables. © *2008 American Institute of Physics*.
[DOI: 10.1063/1.2916718]

I. INTRODUCTION

Conformational transitions are critical to the function of proteins and nucleic acids. These transitions span large ranges of length scales, time scales, and complexity, and include ligand binding,[1] complex conformational rearrangements between native protein substates,[2,3] and folding.[4,5] Understanding these processes is challenging, as they often involve various pathways *via* many intermediate conformations.

A natural approach towards modeling the kinetics of molecules is by partitioning the state space into discrete states.[6–8] In particular, biomolecular function often depends on the ability to undergo transitions between long-lived or "metastable" states,[9] which serve as a useful definition of states in a kinetic model.[7,8]

The switching process between conformational substates is often described with the memoryless Master equation,

$$\frac{dp(t)}{dt} = p(t)K, \tag{1}$$

with $p(t) \in \mathbb{R}^{1\times m}$ containing the probability to find the system in each of its m states at time t. $K \in \mathbb{R}^{m\times m}$ is a rate matrix with K_{ij} being the transition rate from state i to state j, and the diagonal elements are given by $K_{ii}=-\Sigma_{j\neq i}K_{ij}$ in order to ensure mass conservation. Alternatively, the system dynamics can be described by a discrete-time Markov process using the transition matrix, $T(\tau) \in \mathbb{R}^{m\times m}$, whose entries, T_{ij}, provide the probability of the system to be found in state j at time $t+\tau$ given that it was in state i at time t. $T(\tau)$ is row stochastic, i.e., $\Sigma_j T_{ij}=1$ for all i. The time-discrete analog to Eq. (1) is

$$p(k\tau) = p(0)T^k(\tau). \tag{2}$$

Equations (1) and (2) provide equivalent results at discrete times $t=k\tau$, $k \in \mathbb{N}_0$, and are related by $T(\tau)=\exp(\tau K)$.[10] Here, the transition matrix formulation will be used.

The memoryless ansatz implies that the dynamics between states is Markovian at lag time τ. In other words, the state of the system in the next time step, $t+\tau$, is assumed to only depend on the state at the current time t and not on its previous history,

$$p[s(t+\tau)|s(t)] = p[s(t+\tau)|s(t), s(t-\tau), s(t-2\tau), \ldots, s(0)],$$

where $s(t) \in \{1, \ldots, m\}$ indicates the discrete state at time t. In many cases it is not trivial to ensure Markovianity. The boundaries of states and the lag time τ need to be defined appropriately. However, this issue is beyond the scope of the present study and is discussed elsewhere.[7,8]

Usually, $T(\tau)$ is not readily given but needs to be estimated from a set of trajectories that can, e.g., be generated by molecular dynamics simulations. Since these simulations are of finite length, the estimated $T(\tau)$ is associated with

a)Electronic mail: noe@math.fu-berlin.de. Phone: +49 (0)30 838 75354. FAX: +49 (0)30 838 75412.

uncertainty. For a given set of observed transitions from trajectory data, what is the uncertainty of $T(\tau)$ and how does this affect the uncertainty of some function of $T(\tau)$, say $f[T(\tau)]$? This question is addressed in the present paper. Estimating these uncertainties is essential as this allows the reliability of some observable computed from molecular dynamics (MD) simulations to be assessed. Additionally, one may exploit knowledge of these uncertainties by planning new simulations such as to most reduce the uncertainties in the observables of interest, and thus to get the converged observables with a minimal amount of simulation effort.[11–14]

Consider one trajectory with n observations at time resolution τ given by

$$Y=\{y_1=s(0),y_2=s(\tau),\ldots,y_n=s((n-1)\tau)\}.$$

(The generalization to multiple trajectories is straightforward.) Let the frequency matrix $C=(c_{ij})$ count the number of observed transitions between states, i.e., c_{ij} is the number of observed transitions from state i at time t to state j at time $t+\tau$, summed over all times t. In the limit of an infinitely long trajectory, the elements of the true transition matrix are given by the trivial estimator,

$$\hat{T}_{ij}(\tau)=\frac{c_{ij}}{\Sigma_k c_{ik}}=\frac{c_{ij}}{c_i}, \tag{3}$$

where $c_i:=\Sigma_{k=1}^{m}c_{ik}$ is the total number of observed transitions leaving state i. For a trajectory of limited length, the underlying transition matrix $T(\tau)$ cannot be unambiguously computed. The probability that a particular $T(\tau)$ would generate the observed trajectory is given by

$$p(Y|T)=\prod_{k=1}^{n-1}T_{y_k,y_{k+1}}=p(C|T)=\prod_{i,j=1}^{m}T_{ij}^{c_{ij}}.$$

Vice versa, the probability that the observed data was generated by a particular transition matrix $T(\tau)$ is

$$p(T|C)\propto p(T)p(C|T)=p(T)\prod_{i,j\in S}T_{ij}^{c_{ij}}, \tag{4}$$

where $p(T)$ is the prior probability of transition matrices before observing any data. It turns out that $\hat{T}(\tau)$, as provided by Eq. (3), is the maximum of $p(C|T)$ and thus also of $p(T|C)$ when transition matrices are assumed to be uniformly distributed *a priori*. Since $p(T|C)$ is called likelihood, $\hat{T}(\tau)$ is called maximum likelihood estimator. In the limit of infinite sampling, $p(T|C)$ converges towards a delta distribution with its peak at $\hat{T}(\tau)$. When sampling is finite, the uncertainties of the entries of $\hat{T}(\tau)$ may be estimated by the elementwise standard deviations of $p(T|C)$.

In general, one is interested to compute a particular property, $f[T(\tau)]$, from the transition matrix. f may represent any mathematical function, decomposition, or algorithm. As examples, we will consider following properties here:

(1) *The elements* of $T(\tau)$. Here, the diagonal elements T_{ii} are of special interest as they indicate the lifetimes of states. The half-life of state i is given by $h=\log(0.5)/\log(T_{ii})$.

(2) *The free energy differences between states*, A_i, resulting from the probabilities π_i to be in each state in equilibrium. These are obtained from the first eigenvector, q_1, of T as $\pi_i=q_{1i}/\Sigma_{j=1}^{m}q_{1j}$, thus

$$A_i/RT=-\log\frac{q_{1i}}{q_{1r}}, \tag{5}$$

where τ is the reference state.

(3) *The eigenvalues* of $T(\tau)$, $\Lambda=(\lambda_1,\ldots,\lambda_m)$, which indicate the time scales of the transition processes involved: The time scale of the ith transition process is given by

$$\tau_i^*=-\tau/\log(\lambda_i). \tag{6}$$

One is then interested in how the uncertainty of the transition matrix, induced by the distribution $p(T|C)$, carries over to uncertainties in the target function. In other words, for a given observation C, what is the distribution of target functions, $p[f(T|C)]$ and its standard deviation?

An approach suggested in Ref. 11 is based on first-order perturbation theory: The posterior probability (4) is locally approximated by a multivariate Gaussian centered at the maximum $\hat{T}(\tau)$, and the target function $f(T)$ is approximated by a Taylor series truncated after the first term, i.e., $f(T)\approx f(\hat{T})+\nabla f(T)(T-\hat{T})$. The linear approximation of f preserves the Gaussian shape of the distribution, allowing the standard deviation of $f(T)$ to be calculated analytically. While this approach is computationally very efficient, the two approximations involved are in some cases not justified: (i) The Gaussian approximation is relatively poor for states with few outgoing transition counts and permits unphysical values [probabilities <0 or >1, resulting in possibly unphysical values of $f(T)$]. (ii) It is unclear how well the first-order Taylor expansion will perform for various nonlinear functions $f(T)$.

An alternative to first-order perturbation theory is to generate an ensemble of transition matrices, according to the posterior probability (4), to compute the target function $f(T)$ for each sample T, and to thus sample the distribution of $f(T)$. One approach, also suggested in Ref. 11, is to rewrite the posterior probability (4) as

$$p(T|C)=p(T)\prod_{i,j\in S}T_{ij}^{c_{ij}}=\prod_{i\in S}\left[p(T_i)\prod_{j\in S}T_{ij}^{c_{ij}}\right], \tag{7}$$

and when restricting the prior distributions to Dirichlet-formed distributions, $p(T_i)=\Pi_{j\in S}T_{ij}^{\beta_{ij}}$, where β_{ij} are the transition counts assumed to have happened prior to observing any data, resulting in a posterior of

$$p(T|C)=\prod_{i\in S}\prod_{j\in S}T_{ij}^{\beta_{ij}+c_{ij}}, \tag{8}$$

where each factor $\Pi_{j\in S}T_{ij}^{\beta_{ij}+c_{ij}}$ has the form of a Dirichlet distribution. Efficient samplers for the Dirichlet distribution exist (see p. 594 of Ref. 15 and Ref. 16). This approach ensures that all sampled transition matrices are stochastic matrices (constraints C1 and C2 in Table I). Unfortunately, since this approach treats individual rows of T independently,

TABLE I. Constraints for transition matrices.

C1	Elementwise non-negativity	$0 \leqslant T_{ij}$	$\forall i,j$
C2	Stochasticity	$\Sigma_{j=1}^{m} T_{ij} = 1$	$\forall i$
C3	Detailed balance	$\pi_i T_{ij} = \pi_j T_{ji}$	$\forall i,j$
C4	Fixed stationary distribution	$\pi^* = \pi^* T$	π^* constant

it is not well suited to ensure additional properties of T. In particular, since molecular systems in equilibrium fulfill detailed balance, it is desirable to sample only transition matrices that fulfill detailed balance with respect to their stationary distribution π (constraint C3 in Table I). Additionally, in some cases one has prior knowledge of some properties of T, for example, from experiments, which one would like to enforce in the sampling procedure. For example, one may know that T has a particular predefined stationary distribution π^* (constraint C4 in Table I).

Here, a general method to sample transition matrices according to the posterior probability (4) based on Markov chain Monte Carlo (MCMC) is proposed. While it is computationally more expensive than the linear error analysis and the Dirichlet sampling, it is more general than these methods. In particular, it allows (i) the complete distribution of arbitrary observables to be approximated to the desired degree of accuracy, (ii) the sampling to be restricted to transition matrices fulfilling additional constraints, such as detailed balance and predefined π, and (iii) arbitrary prior distributions $p(T)$ to be employed. The method is illustrated on μs MD simulations of a hexapeptide for which the distributions and uncertainties of the free energy differences between conformations, the transition matrix elements and the transition matrix eigenvalues are estimated.

II. SAMPLING STEPS

To sample the distribution (4), a sampling procedure is proposed based on taking Monte Carlo steps in T space: Given a current matrix T and a proposed new matrix T', the acceptance probability is computed by

$$p_{\text{accept}} = \frac{p(T' \to T)}{p(T \to T')} \frac{p(T'|C)}{p(T|C)}, \tag{9}$$

where $p(T \to T')$ and $p(T' \to T)$ denote the probability to propose T' given T and vice versa. Any proposal step can be used to sample the probability $p(T|C)$, provided that two conditions are satisfied:

- $p(T \to T')$ and $p(T' \to T)$ can be evaluated for every possible proposal step, such that (9) can be evaluated.
- The proposal steps generate an ergodic chain, i.e., if $\mathcal{T}$ denotes the set of matrices to be sampled from, then from any matrix $T \in \mathcal{T}$ any other matrix $T' \in \mathcal{T}$ must be accessible with a finite number of steps.

In this section, MCMC sampling steps are constructed that will allow transition matrices to be sampled such that they fulfill stochasticity, detailed balance, or provide a predefined stationary distribution. All acceptance probabilities are given for the case of a uniform prior distribution $p(T)$. However, nonuniform priors can straightforwardly be built into the acceptance probability if desired.

A. Nonreversible element shift

In order to sample transition matrices that do not fulfill detailed balance, the "nonreversible element shift" is introduced, which modifies off-diagonal matrix elements T_{ij} independently of T_{ji}. Stochasticity is preserved by appropriate modification of the diagonal element T_{ii}. This results in the following Monte Carlo step for the corresponding transition matrix:

$$T'_{ij} = T_{ij} - \Delta,$$

$$T'_{ii} = T_{ii} + \Delta.$$

In order to ensure elementwise non-negativity, Δ is drawn uniformly from the range.

$$\Delta \in [-T_{ii}, T_{ij}].$$

The forward and backward proposal probabilities for this step are symmetric,

$$p(T \to T') = \frac{1}{T_{ij} + T_{ii}},$$

$$p(T' \to T) = \frac{1}{T'_{ij} + T'_{ii}} = \frac{1}{T_{ij} - \Delta + T_{ii} + \Delta} = p(T \to T').$$

Acceptance probability is thus given by the ratio of the posterior probabilities,

$$p_{\text{acc}} = \frac{p(T'|C)}{p(T|C)} = \left(\frac{T_{ii} + \Delta}{T_{ii}}\right)^{C_{ii}} \left(\frac{T_{ij} - \Delta}{T_{ij}}\right)^{C_{ij}}.$$

B. Reversible element shift

The "reversible element shift" modifies the opposite off-diagonal matrix elements, T_{ij} and T_{ji}, such that detailed balance is preserved. Stochasticity is preserved by appropriate modification of the diagonal elements T_{ii} and T_{jj}. Consider a pair of states (i,j), $i \neq j$. The changed elements in the proposed transition matrix, T', are given by

$$T'_{ij} = T_{ij} - \Delta,$$

$$T'_{ii} = T_{ii} + \Delta,$$

$$T'_{ji} = T_{ji} - \frac{\pi_i}{\pi_j}\Delta,$$

$$T'_{jj} = T_{jj} + \frac{\pi_i}{\pi_j}\Delta.$$

If T fulfills detailed balance, the stationary distribution remains unchanged ($\pi' = \pi$),

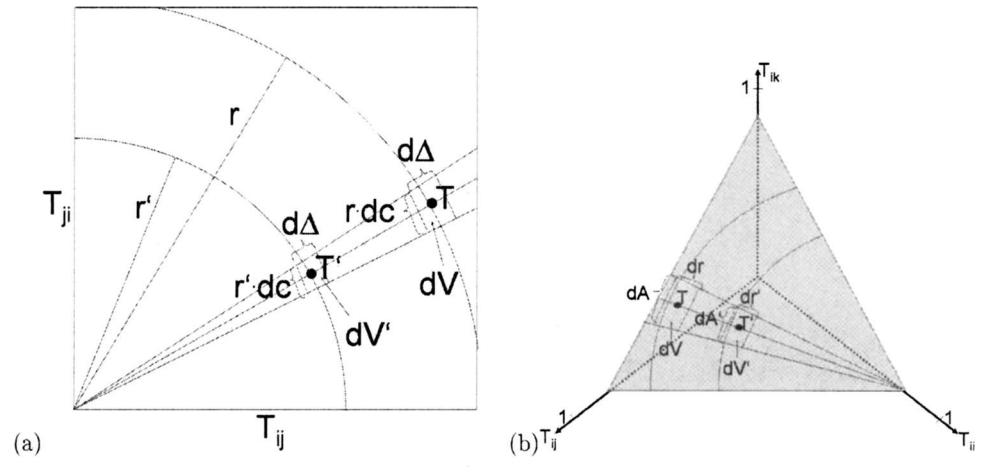

FIG. 1. Schemes illustrating the volume element changes upon reversible element shift (left) and row shift (right).

$$\pi T' = \Bigg[\pi_1, \ldots, \pi_{i-1},$$

$$\pi_1 T_{1i} + \ldots + \pi_i (T_{ii} + \Delta) + \ldots + \pi_j \left(T_{ji} - \frac{\pi_i}{\pi_j} \Delta \right) + \ldots + \pi_m T_{mi}, \pi_{i+1}, \ldots, \pi_{j-1},$$

$$\pi_1 T_{1j} + \ldots + \pi_i (T_{ij} - \Delta) + \ldots + \pi_j \left(T_{jj} + \frac{\pi_i}{\pi_j} \Delta \right) + \ldots + \pi_m T_{mj}, \pi_{j+1}, \ldots, \pi_m \Bigg]$$

$$= [\pi_1, \ldots, \pi_m] = \pi.$$

Furthermore, if T fulfills detailed balance, T' fulfills detailed balance as well,

$$\pi_i' T_{ij}' = \pi_i (T_{ij} - \Delta) = \pi_i T_{ij} - \pi_i \Delta,$$

$$\pi_j' T_{ji}' = \pi_j \left(T_{ji} - \frac{\pi_i}{\pi_j} \Delta \right) = \pi_j T_{ji} - \pi_i \Delta.$$

Thus,

$$\pi_i T_{ij} = \pi_j T_{ji} \Rightarrow \pi_i' T_{ij}' = \pi_j' T_{ji}'.$$

To obtain the permitted range of Δ, consider the following constraints:

$$\text{(a)} \quad T_{ii}' = T_{ii} + \Delta \geqslant 0 \quad \rightarrow \quad \Delta \geqslant -T_{ii},$$

$$\text{(b)} \quad T_{jj}' = T_{jj} + \Delta \frac{\pi_i}{\pi_j} \geqslant 0 \quad \rightarrow \quad \Delta \geqslant -\frac{\pi_j}{\pi_i} T_{jj},$$

$$\text{(c)} \quad T_{ij}' = T_{ij} - \Delta \geqslant 0 \quad \rightarrow \quad \Delta \leqslant T_{ij},$$

$$\text{(d)} \quad T_{ji}' = T_{ji} - \Delta \frac{\pi_i}{\pi_j} \geqslant 0 \quad \rightarrow \quad \Delta \leqslant \frac{\pi_j}{\pi_i} T_{ji}.$$

Constraint (d) is redundant with (c) for matrices fulfilling detailed balance. Consequently, Δ is drawn uniformly from the following range:

$$\Delta \in \left[\max\left(-T_{ii}, -\frac{\pi_j}{\pi_i} T_{jj} \right), T_{ij} \right].$$

The proposal probabilities are symmetric along the line parametrized by Δ,

$$p(T \rightarrow T') = \frac{1}{T_{ij} - \max\left(-T_{ii}, -\frac{\pi_j}{\pi_i} T_{jj} \right)},$$

$$p(T' \rightarrow T) = \frac{1}{T_{ij} - \max\left(-T_{ii} - \Delta, -\frac{\pi_j}{\pi_i} \left(T_{jj} - \frac{\pi_i}{\pi_j} \Delta \right) \right)}$$

$$= -p(T \rightarrow T'),$$

such that the proposal probability is identical to 1,

$$p_{\text{prop}} = 1.$$

If the reversible element shift is combined with another step that allows to move between different π, the proposal probability needs to incorporate the fact that the different reversible element shifts for a given (i,j) pair are not orthogonal [see Fig. 1(a)]. In this case, the reversible element shift changes the size of a volume element proportional to the distance of (T_{ij}, T_{ji}) from (0,0), here denoted by r,

$$dV = d\Delta \cdot (r \cdot dc),$$

$$dV' = d\Delta \cdot (r' \cdot dc),$$

$$p_{\text{prop}} = \frac{p(T' \to T)}{p(T \to T')} = \frac{r'}{r} = \sqrt{\frac{(T_{ij}-\Delta)^2 + (T_{ji} - (\pi_i/\pi_j)\Delta)^2}{(T_{ij})^2 + (T_{ji})^2}}.$$

Acceptance probability:

$$p_{\text{acc}} = p_{\text{prop}} \frac{p(T'|C)}{p(T|C)} = p_{\text{prop}} \left(\frac{T_{ii}+\Delta}{T_{ii}}\right)^{C_{ii}} \left(\frac{T_{ij}-\Delta}{T_{ij}}\right)^{C_{ij}} \left(\frac{T_{jj}+(\pi_i/\pi_j)\Delta}{T_{jj}}\right)^{C_{jj}} \times \left(\frac{T_{ji}-(\pi_i/\pi_j)\Delta}{T_{ij}}\right)^{C_{ji}}.$$

Here, p_{prop} is 1 or r'/r, when sampling with fixed π or with changing π, respectively.

C. Row shift

Finally, a step is considered which scales the self-transition probability T_{ii} and all outgoing transition probabilities T_{ij} as follows:

$$T'_{ij} = \alpha T_{ij},$$

$$T'_{ii} = 1 - \sum_{k\neq i} T'_{ik} = 1 - \alpha \sum_{k\neq i} T_{ik} = 1 - \alpha(1 - T_{ii}) = \alpha T_{ii} - \alpha + 1.$$

The step thus changes the ith row of T. The parameter α is subject to the following constraints:

(a) $\alpha T_{ij} \geqslant 0 \quad \rightarrow \quad \alpha \geqslant 0,$
(b) $\alpha T_{ii} - \alpha + 1 \leqslant 1 \quad \rightarrow \quad \alpha \geqslant 0,$
(c) $\alpha T_{ii} - \alpha + 1 \geqslant 0 \quad \rightarrow \quad \alpha \leqslant 1/(1 - T_{ii}),$
(d) $\alpha T_{ij} \leqslant 1 \ \ \forall\, j \neq i \quad \rightarrow \quad \alpha \leqslant 1/\max(T_{ij}) \ \ \forall\, j \neq i.$

Note that $(1-T_{ii}) \geqslant T_{ij}$ for all $j \neq i$, and thus $(1-T_{ii})^{-1} \leqslant (\max(T_{ij}))^{-1}$, making (d) redundant with (c). Consequently, α is drawn uniformly from following range:

$$\alpha \in \left[0, \frac{1}{1-T_{ii}}\right].$$

The ratio of proposal probabilities is given by

$$\frac{p(T' \to T)}{p(T \to T')} = \frac{p_\alpha(T' \to T)}{p_\alpha(T \to T')} \frac{dA'}{dA} = \frac{dr'dA'}{drdA},$$

where p_α is the proposal probability along the line parametrized by α, while dA is an area element orthogonal to that line and intersecting with T, and dA' is the scaled area element [see Fig. 1(b)]. With $p(\alpha) = 1 - T_{ii}$ and $\alpha = T'_{ij}/T_{ij} = (1-T'_{ii})/(1-T_{ii})$, we obtain

$$p_\alpha(T_{ij} \to T'_{ij}) = p(\alpha) \left|\frac{\partial \alpha}{\partial T'_{ij}}\right| = (1 - T_{ii}) \frac{1}{T_{ij}},$$

$$p_\alpha(T_{ii} \to T'_{ii}) = p(\alpha) \left|\frac{\partial \alpha}{\partial T'_{ii}}\right| = (1 - T_{ii}) \frac{1}{1 - T_{ii}} = 1,$$

$$p_\alpha(T'_{ij} \to T_{ij}) = p(\alpha') \left|\frac{\partial \alpha'}{\partial T_{ij}}\right| = (1 - T'_{ii}) \frac{1}{T'_{ij}} = \alpha(1 - T_{ii}) \frac{1}{\alpha T_{ij}} = p(T_{ij} \to T'_{ij}),$$

$$p_\alpha(T'_{ii} \to T_{ii}) = p(\alpha') \left|\frac{\partial \alpha'}{\partial T_{ii}}\right| = (1 - T'_{ii}) \frac{1}{1 - T'_{ii}} = \alpha(1 - T_{ii}) \frac{1}{\alpha(1 - T_{ii})} = 1 = p(T_{ii} \to T'_{ii}).$$

Thus, $p_\alpha(T' \to T)/p_\alpha(T \to T') = 1$. The area element is proportional to the $(m-2)$th power of the distance of the ith row from $(0, \ldots, 0, T_{ii} = 1, 0, \ldots, 0)$, denoted by r,

$$dA \propto (r \cdot dc)^{(m-2)},$$

$$dA' \propto (r' \cdot dc)^{(m-2)}.$$

With

$$r = \sqrt{(1 - T_{ii})^2 + \Sigma_{j\neq i} T_{ij}^2}$$

and

$$r' = \sqrt{\alpha^2(1 - T_{ii})^2 + \Sigma_{j\neq i} \alpha^2 T_{ij}^2} = \alpha r,$$

one obtains

$$\frac{p(T' \to T)}{p(T \to T')} = \alpha^{(m-2)}.$$

Acceptance probability:

$$p_{\text{acc}} = \frac{p(T' \to T)}{p(T \to T')} \frac{p(T'|C)}{p(T|C)} = \alpha^{(m-2)} \left(\frac{T'_{ii}}{T_{ii}}\right)^{C_{ii}} \prod_{j\neq i} \left(\frac{T'_{ij}}{T_{ij}}\right)^{C_{ij}} = \alpha^{(m-2)} \left(\frac{1 - \alpha(1 - T_{ii})}{T_{ii}}\right)^{C_{ii}} \prod_{j\neq i} \alpha^{C_{ij}} = \alpha^{(m-2+C_i-C_{ii})} \left(\frac{1 - \alpha(1 - T_{ii})}{T_{ii}}\right)^{C_{ii}},$$

with $C_i = \Sigma_{j=1}^m C_{ij}$. The row shift would be ineffective once any T_{ij} becomes identical 0. However, the acceptance probability is such that this does not occur during the sampling,

$$\alpha \to 0 \Rightarrow p_{\text{acc}} \to 0,$$

$$\alpha \to \frac{1}{1 - T_{ii}} \Rightarrow p_{\text{acc}} \to 0.$$

The row shift operation will change the stationary distribution π. π is, for example, required to conduct the revers-

ible element shifts. Instead of recomputing the stationary distribution expensively by solving an eigenvalue problem, it may be efficiently updated as follows:

$$\pi_i' = \frac{\pi_i}{\pi_i + \alpha(1-\pi_i)},$$

$$\pi_j' = \frac{\alpha\pi_j}{\pi_i + \alpha(1-\pi_i)}.$$

Proof.

$$\pi' = \pi' T'$$

has the elements π_i and π_j, $j \neq i$, given by

$$\pi_i' = \pi_1' T_{1i}' + \ldots + \pi_{i-1}' T_{i-1,i}' + \pi_i' T_{ii}' + \pi_{i+1}' T_{i+1,i}' + \ldots + \pi_m' T_{mi}',$$

$$\frac{\pi_i}{\pi_i + \alpha(1-\pi_i)} = \frac{\alpha\pi_1 T_{1i} + \ldots + \alpha\pi_{i-1} T_{i-1,i} + \pi_i[1-\alpha(1-T_{ii})] + \alpha\pi_{i+1} T_{i+1,i} + \ldots + \alpha\pi_m T_{mi}}{\pi_i + \alpha(1-\pi_i)},$$

$$\pi_i = \alpha[\pi_1 T_{1i} + \ldots + \pi_m T_{mi}] + \pi_i - \alpha\pi_i,$$

$$\pi_i = \pi_1 T_{1i} + \ldots + \pi_m T_{mi},$$

and

$$\pi_j' = \pi_1' T_{1j}' + \ldots + \pi_{i-1}' T_{i-1,j}' + \pi_i' T_{ij}' + \pi_{i+1}' T_{i+1,j}' + \ldots + \pi_m' T_{mj}',$$

$$\frac{\alpha\pi_j}{\pi_i + \alpha(1-\pi_i)} = \frac{\alpha\pi_1 T_{1j} + \ldots + \alpha\pi_{i-1} T_{i-1,j} + \pi_i \alpha T_{ij} + \alpha\pi_{i+1} T_{i+1,j} + \ldots + \alpha\pi_m T_{mj}}{\pi_i + \alpha(1-\pi_i)},$$

$$\pi_j = \pi_1 T_{1j} + \ldots + \pi_m T_{mj}.$$

Thus,

$$\pi = \pi T \Leftrightarrow \pi' = \pi' T'.$$

D. Energy landscape interpretation

There is a straightforward physical interpretation of the previous Monte Carlo steps. Imagine a discrete energy landscape with m states having energies E_i and $m(m-1)$ transition states between different states i,j having energies E_{ij}. All energies are normalized by "measuring" them in units of RT. This model is translated into a transition matrix by considering the transition $i \to j$ as a Markov jump process with a Metropolis probability depending on the energy barrier,

$$T_{ij} = \begin{cases} \exp(-E_{ij} + E_i), & i \neq j, \\ 1 - \sum_{k \neq i} T_{ik}, & i = j. \end{cases}$$

As a consequence of this definition the following relationships between the transition matrix and the energy model are obtained:

(1) Detailed balance is defined for both systems and manifests itself as

$$\pi_i T_{ij} = \pi_j T_{ji},$$

$$\exp(-E_i)\exp(-E_{ij} + E_i) = \exp(-E_j)\exp(-E_{ji} + E_i),$$

$$E_{ij} = E_{ji}.$$

(2) If detailed balance holds, then $\pi_i = \exp(-E_i)/\Sigma_k \exp(-E_k)$ (Boltzmann distribution).

(3) If detailed balance holds and one state energy is fixed (e.g., $E_1 = 0$), then the map between the energy model and T is bijective.

(4) The constraint for stochasticity, $\Sigma_{k \neq i} T_{ik} \leqslant 1$, corresponds to $\exp(E_i)\Sigma_{j=1}^m \exp(-E_{ij}) \leqslant 1$ or $\Sigma_{j=1}^m \exp(-E_{ij}) \leqslant \exp(-E_i)$ in the energy model. The necessary condition $T_{ik} \leqslant 1 \; \forall k \in (1 \ldots m)$ corresponds to $E_{ik} \geqslant E_i \; \forall k \in (1 \ldots m)$, i.e., the energy of the transition state $i \to j$ must be at least as high as the energy of state i.

Shifting an off-diagonal element i,j of the transition matrix by $-\Delta$ has the following effect in the energy model:

$$T_{ij}' = T_{ij} - \Delta = T_{ij}\exp(-dE) = \exp[-(E_{ij} + dE - E_i)],$$

and thus corresponds to shifting the energy of the transition state by $dE := -\log(1 - \Delta/T_{ij})$. For the reversible element shift, we also have $T_{ji}' = T_{ji} - \Delta\pi_i/\pi_j = \exp[-(E_{ji} + dE - E_j)]$, thus the forward and backward transition state is shifted in the same way and $E_{ij} = E_{ji}$ is maintained. The nonreversible and reversible element shifts thus correspond to manipulating the barriers in the energy model. It is thus obvious from an energetic point of view that the stationary distribution is conserved when using the reversible element shift as it leaves the state energies and thus the Boltzmann distribution untouched.

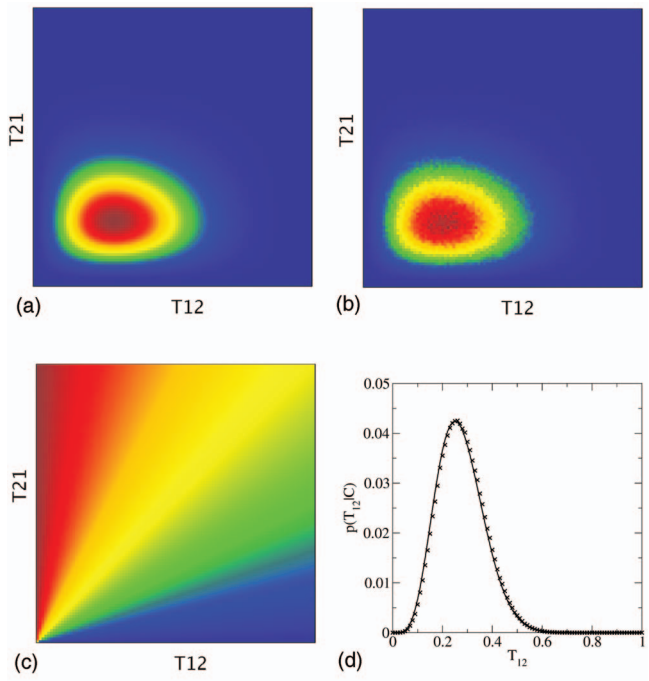

FIG. 2. (Color) Illustration of sampling of transition probability matrices for the observation $C=\left(\begin{smallmatrix}5 & 3\\ 2 & 10\end{smallmatrix}\right)$. Panels (a), (b), and (c) show the probability distribution on the off-diagonal matrix elements. The color encodes the probability density, with blue=0 and red=1. Each density was scaled such that its maximum is equal to 1. (a) Analytic density of stochastic matrices. (b) Sampled density of stochastic matrices (these matrices automatically fulfill detailed balance). (c) Stationary probability of the first state π_1. When sampling with respect to a fixed stationary probability distribution π^*, the ensemble is fixed to the line $T_{21}=T_{12}\pi_1^*/(1-\pi_1^*)$. (d) Sampled and exact density of T_{12} of reversible matrices with fixed stationary distribution $\pi^*=(0.5,0.5)$.

In the row shift operation,

$$T'_{ij}=\alpha T_{ij}=\exp(dE)T_{ij}=\exp[-(E_{ij}-(E_i+dE))],$$

the energy of state i can be imagined to be shifted by $dE:=\log(\alpha)$.

III. TRANSITION MATRIX SAMPLING

A. Stochastic matrices

Consider the ensemble of T matrices which fulfill the constraints of elementwise non-negativity (C1) and stochasticity (C2) constraints. The sampling is initialized with the maximum likelihood estimator [Eq. (3)] and uses the nonreversible element shift operation as specified by Algorithm 1.

Algorithm 1. Metropolis Monte Carlo sampling of stochastic matrices.

Input: Transition count matrix $C\in\mathbb{N}_0^{m\times m}$.
Number of samples N.

Output: Ensemble of transition matrices, $T_1\ldots,T_N$.

1. Initialize $T_{0,ij}=C_{ij}/\Sigma_{k=1}^m C_{ik}\forall i,j\in(1,\ldots,m)$.
2. For $n=1\ldots N$.
   2.1 Generate uniform random variables: $i,j\in\{1,\ldots,m\}$, $\Delta\in[-(T_{n-1})_{ii},(T_{n-1})_{ij}]$, $r\in[0,1]$.
   2.2 $T_n:=T_{n-1}$.
   2.3 Nonreversible element shift:
   $$p_{\mathrm{acc}}:=\left(\frac{(T_n)_{ii}+\Delta}{(T_n)_{ij}}\right)^{C_{ii}}\left(\frac{(T_n)_{ij}-\Delta}{(T_n)_{ij}}\right)^{C_{ij}}$$
   2.4 If $r\leqslant p_{\mathrm{acc}}$:
   Increment $(T_n)_{ii}$ by Δ,
   Decrement $(T_n)_{ij}$ by Δ.

Ergodicity. In order to show that the nonreversible element shift generates an ergodic Markov chain, consider two arbitrary transition matrices T and T'. Since the rows are changed independently of each other, it suffices to concentrate on one particular row, $T_i=(T_{i1},\ldots,T_{im})$ and $T'_i=(T'_{i1},\ldots,T'_{im})$. To transform T_i into T'_i, the following sequence of steps may be used:

(1) For all $j\neq i$, do nonreversible element shift with $\Delta=T_{ij}$.
(2) For all $j\neq i$, do nonreversible element shift with $\Delta=-T'_{ij}$.

Part 1 has $m-1$ steps and results in a row $(0,\ldots,0,T_{ii}=1,0,\ldots,0)$. Part 2 has also $m-1$ steps and results in the row T'_i. This procedure can be repeated for every other row. Thus, any two transition matrices T and T' can be transformed into one another by at most $2m(m-1)$ steps.

Example 1. Figure 2 illustrates the sampling procedure by visualizing the distribution of off-diagonal elements of a 2×2 transition matrix for the observed transition counts

$$C=\begin{pmatrix}5 & 2\\ 3 & 10\end{pmatrix}.$$

The analytic probability distribution $p(T|S)=(1-T_{12})^5(T_{12})^2(T_{21})^3(1-T_{22})^{10}$ (panel a) is compared to the distribution sampled with Algorithm 1 (panel b), indicating the correctness of the sampling procedure.

Example 2. Figure 3 illustrates the sampling procedure on a 3×3 transition matrix for the observed transition counts

$$C=\begin{pmatrix}8 & 2 & 1\\ 2 & 10 & 3\\ 2 & 3 & 6\end{pmatrix}.$$

The sampled distribution is visualized by three marginal distributions: T_{12} and T_{13} (panel b), T_{21} and T_{23} (panel e), and T_{31} and T_{32} (panel h). For comparison, the analytic distributions are shown in panels a, d, and g.

B. Reversible stochastic matrices

Consider the ensemble of T matrices which fulfill the constraints of elementwise non-negativity (C1), stochasticity (C2), and detailed balance (C3). The sampling is initialized with the reversible matrix,

$$T_{ij}=\frac{1}{2}\frac{C_{ij}+C_{ji}}{\Sigma_{k=1}^m C_{ik}},$$

and uses the reversible element shift and row shift operations, as specified by Algorithm 2.

Algorithm 2. Metropolis Monte Carlo sampling of reversible stochastic matrices.
Input: Transition count matrix $C \in \mathbb{N}_0^{m\times m}$. Number of samples N.
Output: Ensemble of reversible transition matrices, $T_1, \ldots, T_N$.
1. Initialize $T_{0,ij}=(C_{ij}+C_{ji})/(2\Sigma_{k=1}^{m} C_{ik})\,\forall\, i,j \in (1,\ldots,m)$.
2. Compute π as stationary distribution of T_0 by solving $\pi=\pi T_0$.
3. For $n=1\ldots$N.
   3.1. Generate uniform random variables: $r_1, r_2 \in [0,1]$.
   3.2. $T_n := T_{n-1}$.
   3.3. If $(r_1 < 0.5)$ Reversible element shift:
      3.3.1. Generate uniform random variables:
      $i,j \in \{1,\ldots,m\}$,
      $\Delta \in \left[\max\left(-(T_{n-1})_{ii}, -\frac{\pi_j}{\pi_i}(T_{n-1})_{jj}, (T_{n-1})_{ij} \right. \right.$.
      3.3.2.
$$p_{\mathrm{acc}} := \left(\frac{((T_n)_{ij}-\Delta)^2 + \left((T_n)_{ji} - \frac{\pi_i}{\pi_j}\Delta\right)^2}{((T_n)_{ij})^2 + ((T_n)_{ji})^2} \right) \left(\frac{(T_n)_{ii}+\Delta}{(T_n)_{ii}} \right)^{C_{ii}} \left(\frac{(T_n)_{ij}-\Delta}{(T_n)_{ij}} \right)^{C_{ij}} \left(\frac{(T_n)_{jj}+\frac{\pi_i}{\pi_j}\Delta}{(T_n)_{jj}} \right)^{C_{jj}} \left(\frac{(T_n)_{ji}-\frac{\pi_i}{\pi_j}\Delta}{(T_n)_{ji}} \right)^{C_{ji}}$$
      3.3.3. If $(r_2 \leqslant p_{\mathrm{acc}})$:
      Increment $(T_n)_{ii}$ by Δ and $(T_n)_{jj}$ by $\Delta\pi_i/\pi_j$.
      Decrement $(T_n)_{ij}$ by Δ and $(T_n)_{ji}$ by $\Delta\pi_i/\pi_j$.
      else Row shift:
      3.3.4. Generate uniform random variables: $i \in (1,\ldots,m)$, $\alpha \in [0, 1/1-T_{ii}]$.
      3.3.5. $p_{\mathrm{acc}} := \alpha^{(m-2+C_i-C_{ii})} \left(\frac{1-\alpha(1-T_{ii})}{T_{ii}} \right)^{C_{ii}}$
      3.3.6. If $r_2 \leqslant p_{\mathrm{acc}}$: For all $j \neq i$: $(T_n)_{ij} = \alpha (T_n)_{ij}$.
$$(T_n)_{ii} = 1 - \Sigma_{j\neq i}(T_n)_{ij}$$
      3.3.7. Update stationary distribution:
      For all $j \neq i$:
      $\pi_j := \alpha\pi_j$
      $\pi_i := 1-\Sigma_{j\neq i}\pi_j$.

Ergodicity. Consider two arbitrary reversible transition matrices, T and T' as well as the corresponding matrices of absolute (unconditional) transition probabilities, defined as $P_{ij}=T_{ij}\pi_i$ and $P'_{ij}=T'_{ij}\pi'_i$. Since T and T' are reversible, P and P' are symmetric. The following steps transform T into T':

(1) For all $i=(1\ldots m-1)$ and $j>i$: Do reversible element shift with $\Delta=-T_{ij}$. In the corresponding P matrix, each such reversible element shift generates $P_{ij}=P_{ji}=0$, $P_{ii} := P_{ii}+P_{ij}$, $P_{jj} := P_{jj}+P_{ij}$. This results in a unit transition matrix $T''=\mathrm{diag}(1,\ldots,1)$.
(2) For all $i=(1\cdots m-1)$ and $j>i$: Do reversible element shift with $\Delta=T'_{ij}$. This results in T'.

Thus, it is possible to transform T into T' in at most $2m(m-1)$ reversible element shifts. Note that, although this proof works with reversible element shifts only, in practice the row shift operation is indispensible in order to guarantee an acceptable convergence rate.

Example 1. Every 2×2 transition matrix is reversible: The first left eigenvector of a 2×2 transition matrix is given by $(1, T_{12}/T_{21})$. When scaled such that its elements sum to 1, it yields the stationary distribution,

$$\pi = \left(\frac{T_{12}}{T_{12}+T_{21}}, \frac{T_{21}}{T_{12}+T_{21}} \right),$$

such that detailed balance is always fulfilled. Indeed, for 2×2 matrices, Algorithm 1 generates the same distribution as Algorithm 2 [see Fig. 2(b)].

Example 2. Figure 3 illustrates how the distribution of a

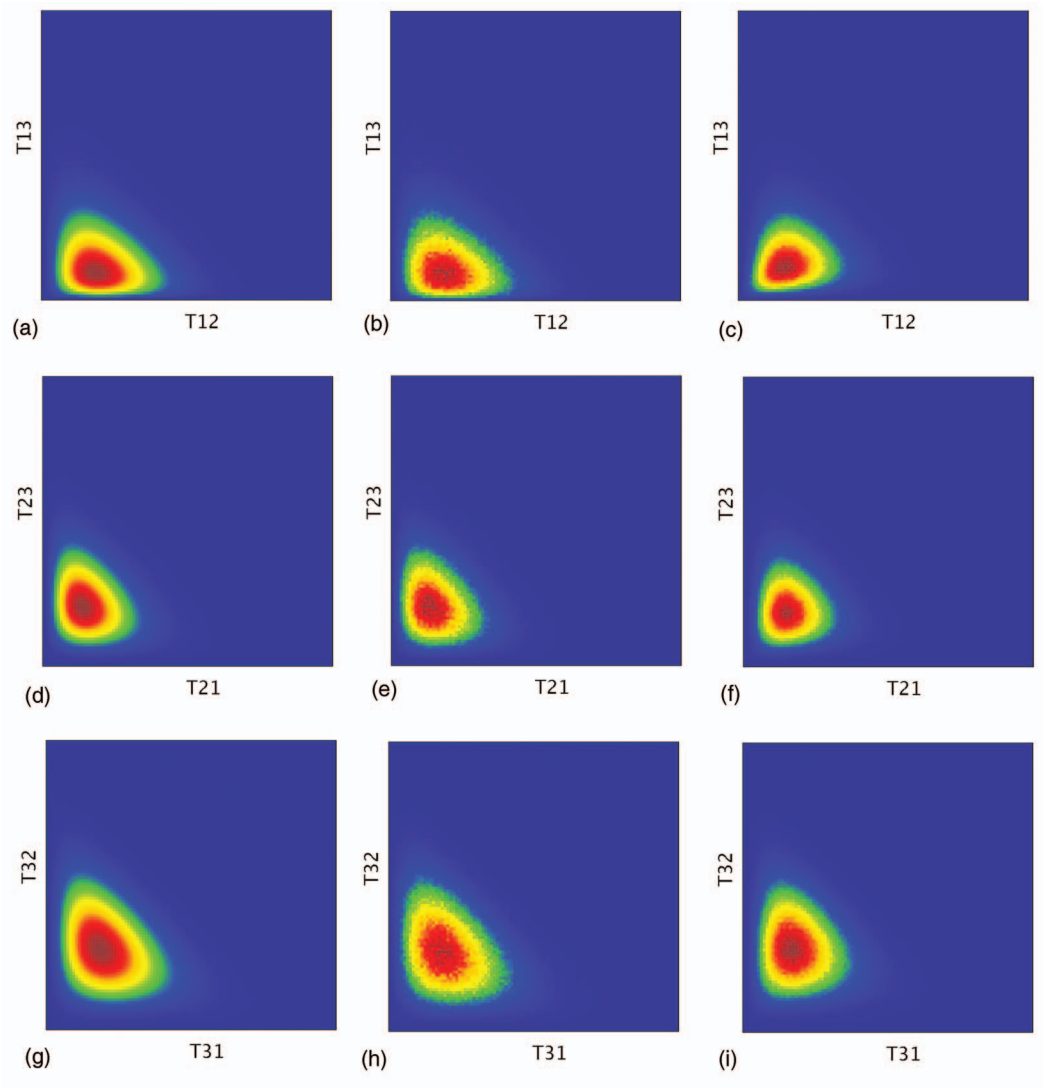

FIG. 3. (Color) Visualization of the probability density of transition matrices to the observation $C=\begin{pmatrix} 8 & 2 & 1 \\ 2 & 10 & 3 \\ 2 & 3 & 6 \end{pmatrix}$. Different two-dimensional marginal distributions are shown in the rows. The analytic and sampled distributions for stochastic matrices are shown in columns 1 and 2, respectively. Column 3 shows the sampled distribution for stochastic matrices fulfilling detailed balance.

3×3 transition matrix differs between the nonreversible (panels b, e, and h) and reversible (panels c, f, and i) cases. For the matrix studied here, the distribution of reversible matrices is slightly narrower.

C. Reversible stochastic matrices with fixed stationary distribution

Consider the ensemble of T matrices which fulfill the constraints of elementwise non-negativity (C1), stochasticity (C2), detailed balance (C3), and generate a predefined stationary distribution π^* (C4). In order to find an initial matrix fulfilling these constraints, the fact is exploited that for a $m\times m$ tridiagonal transition matrix, the stationary distribution π fulfills the equation

$$\frac{\pi_i}{\pi_{i+1}} = \frac{T_{i+1,i}}{T_{i,i+1}}.$$

Also, such a matrix at the same time obeys detailed balance. A valid initial matrix is then generated by Algorithm 3:

Algorithm 3. Initial reversible transition matrix with given stationary distribution π.

1. For $i=(1\ldots m-1)$:
   $T_{i,i+1} := 1$,
   $T_{i+1,i} := \frac{\pi_i}{\pi_{i+1}} T_{i,i+1}$.
2. $c := \max\{\Sigma_{j=1}^{m} T_{ij} | i=1\ldots m\}$.
3. For $i,j=(1\ldots m): T_{ij} := T_{ij}/2c$.
4. For $i=(1\ldots m): T_{ii} := 1-\Sigma_{j\neq i} T_{ij}$.

Since this way of constructing an initial matrix does not take observed transition counts into account, it may be rather far off the peak of the distribution. Thus, it is recommended to ignore the first $10m^2$ samples (five times the maximum ergodicity length, see proof below) from the resulting ensemble. The sampling uses the reversible element shift operation, and is specified by Algorithm 4.

Algorithm 4. Metropolis Monte Carlo sampling of reversible stochastic matrices.

Input: Transition count matrix $C \in \mathbb{N}_0^{m\times m}$.
Desired stationary distribution π.
Number of samples N.

Output: Ensemble of reversible transition matrices with stationary distribution $\pi, T_1, \ldots, T_N$.

1. Initialize T_0 with Algorithm 3.
2. For $n=1 \ldots N$.
   2.1. Generate uniform random variables:

$$r \in [0,1], i,j \in \{1, \ldots, m\},$$

$$\Delta \in \left[\max\left(-(T_{n-1})_{ii}, -\frac{\pi_j}{\pi_i}(T_{n-1})_{jj} \right), (T_{n-1})_{ij} \right].$$

   2.2. $T_n := T_{n-1}$,
   2.3. Row shift:

$$p_{\mathrm{acc}} := \left(\frac{(T_n)_{ii}+\Delta}{(T_n)_{ii}} \right)^{C_{ii}} \left(\frac{(T_n)_{ij}-\Delta}{(T_n)_{ij}} \right)^{C_{ij}} \times \left(\frac{(T_n)_{jj}+\frac{\pi_i}{\pi_j}\Delta}{(T_n)_{jj}} \right)^{C_{jj}} \left(\frac{(T_n)_{ji}-\frac{\pi_i}{\pi_j}\Delta}{(T_n)_{ji}} \right)^{C_{ji}}.$$

   2.4. If $(r < p_{\mathrm{acc}}$:
   Increment $(T_n)_{ii}$ by Δ
   and $(T_n)_{jj}$ by $\Delta\pi_i/\pi_j$.
   Decrement $(T_n)_{ij}$ by Δ
   and $(T_n)_{ji}$ by $\Delta\pi_i/\pi_j$.

Ergodicity. The above algorithm generates an ergodic Markov chain. The ergodicity proof for reversible matrices with arbitrary π (Sec. III B) serves as a proof for fixed π as well.

Example. Figure 2(c) shows the stationary probability π_1 for transition matrices with the observation

$$C = \begin{pmatrix} 5 & 2 \\ 3 & 10 \end{pmatrix}.$$

When fixing π_1 (and thus π) to one particular value, one restricts the density shown in panel (a) to the line $T_{21} = [\pi_1/(1-\pi_1)]T_{12}$. Panel (d) shows the sampled and exact densities for the fixed stationary distribution $\pi=(0.5,0.5)$ along T_{12}.

IV. APPLICATION TO MOLECULAR DYNAMICS

In order to illustrate the transition matrix sampling on a realistic example, a 1 μs MD simulation of the synthetic hexapeptide MR121-GSGSW peptide[17] is used. The simulation was performed in explicit water at 293 K with the GROMACS software package[18] using the GROMOS96 force field[19] (see Appendix A for the detailed simulation protocol). During this simulation, the peptide frequently folds and unfolds and visits various different conformations. Based on this simulation data, the state space was clustered into 34 conformations whose interconversion is well described by a Markov model with a lag time of $\tau=1$ ns (see Appendix B for a detailed description of the clustering and the Markov model). By counting the transitions between metastable conformations at time intervals of 1 ns along the trajectory, the transition count matrix, $C \in \mathbb{N}_0^{34\times 34}$ is obtained which serves as a test case for the sampling procedure.

A. Convergence of transition matrix sampling

Since the algorithms presented here sample the distribution of transition matrices, the question how well the distribution is approximated for a given number of samples, or how many samples are necessary to consider the estimated distribution as converged, arises. To study this, the distribution of transition matrices implied by C was sampled with Algorithm 1. This is the "worst" case in terms of sampling convergence—including the constraints detailed balance (Algorithm 2) and fixed π (Algorithm 4) reduces the number of degrees of freedom. To evaluate the convergence of the estimated distribution of transition matrices, the convergence of the second moment (standard deviation) of several observables was monitored. The following observables were chosen: (i) T_{11} and T_{mm}, i.e., the self-transition probabilities, here corresponding to the least and most populated states, respectively, (ii) eigenvalues λ_2, λ_3, and λ_4 of T, indicating the three slowest time scales of the system, and (iii) the free energy differences of states 1 and $m-1$ with respect to state m, here corresponding to the least and second-most populated states.

Since a single nonreversible element move only changes at most two matrix elements, subsequently generated transition matrices are highly correlated. For this, a matrix is recorded and considered as a "sample" after every 10^4 moves. For each sample step t the values of the aforementioned observables are computed as well as their running means μ_t and standard deviations σ_t. For this, the following update rules were used:

$$\mu_t = \frac{(t-1)\mu_{t-1} + x_t}{t},$$

$$\sigma_t^2 = \frac{(t-1)\sigma_{t-1}^2 + (x_t - \mu_t)(x_t - \mu_{t-1})}{t},$$

where x is the observable. As apparent from Fig. 4, the variance can be considered as converged after about 1000 samples, corresponding to 10^7 moves. This takes approximately 20 s of CPU time on a 1.8 GHz Intel single core, including the time required to compute the observables (such

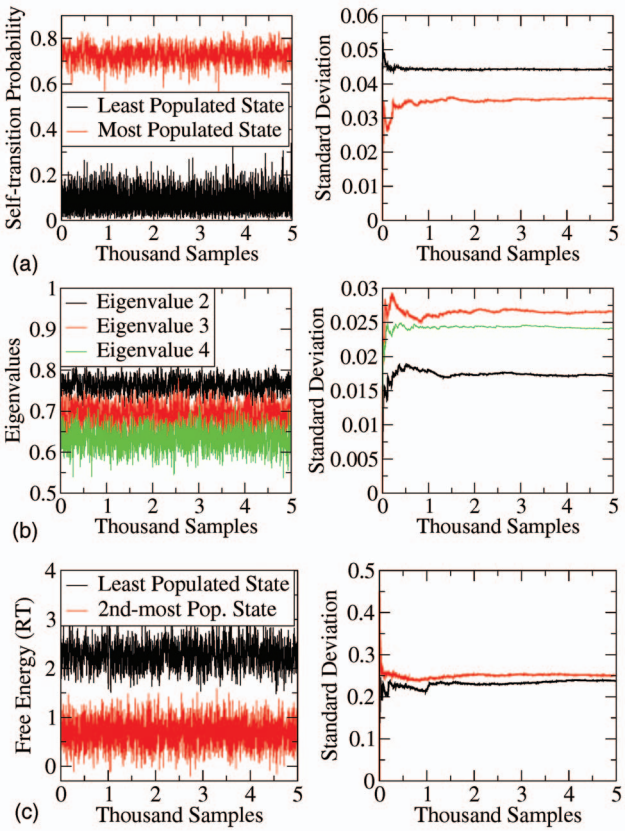

FIG. 4. (Color) Convergence of the transition matrix sampling Algorithm 1. One sample every 10^4 moves was recorded and the convergence is shown for 5000 samples in total. The left panels show the values, for each sample, of (a) the self-transition probabilities of states 1 and m, (b) eigenvalues 2, 3, and 4, and (c) the free energy differences of states 1 and $m-1$ with respect to state m. The right panels show the current estimate for the standard deviation of each of these observables. The standard deviation can be considered converged after about 1000 samples (10^7 moves).

as solving an eigenvalue problem for every sample in the case of free energies). For all computations in the subsequent section, 2000 samples were used.

B. Uncertainty in molecular dynamics simulation

The methods presented here were applied to estimate the uncertainties, i.e., standard deviations of the distributions, of several observables computed from the peptide molecular dynamics simulation.

First, the effect of simulation length on the uncertainties of T itself is studied. For this, segments of the complete 1 μs trajectory were considered, starting at time 0 and having lengths between 10 and 1000 ns. For each segment, the transitions between states were counted using always the same definition of states. For each C matrix obtained in this way, the T matrices were sampled without and with the detailed balance constraint as well as with the stationary distribution π fixed to the one associated with the maximum likelihood transition matrix [Eq. (3)] of the complete trajectory. Figure 5 shows the mean uncertainties of the diagonal elements in panel (a) and the off-diagonal elements in panel (b). The uncertainties decay approximately with inverse power laws, those of the off-diagonal elements decay roughly like an inverse square root. The latter observation is expected for a

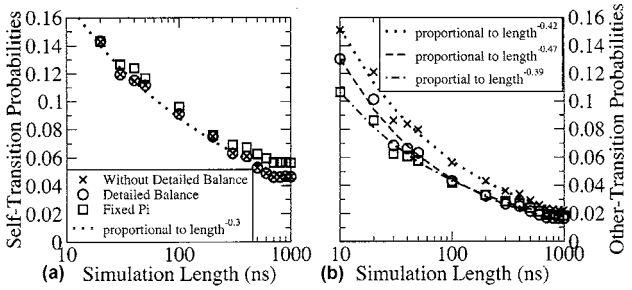

FIG. 5. Mean uncertainties of (a) the diagonal and (b) the off-diagonal elements of the transition matrix for different simulation lengths. The uncertainties are shown for the ensembles of transition matrices, transition matrices with detailed balance, and for a fixed stationary distribution.

Markov model, since transition events are statistically independent after the slowest equilibration time of the system. For the diagonal elements, sampling with or without detailed balance does not provide a significant difference. This is also to be expected, since detailed balance constrains the ratio of symmetric off-diagonal elements, while diagonal elements are not directly affected. For the off-diagonal elements, introducing detailed balance significantly reduces the uncertainties: Approximately half the simulation time is sufficient to obtain a given uncertainty when detailed balance is considered.

Next, the effect of simulation length and constraints on the uncertainties on properties derived from the transition matrix are analyzed. First, consider the free energy differences with respect to the starting state of the simulation (the starting state is chosen in order to have the same reference state for all segments—the number of found states increases when increasing the simulation length). The free energies were computed for each sample T using Eq. (5). As apparent from Fig. 6, the mean uncertainties of the A_i roughly decay according to an inverse power law. Introducing detailed balance only has a very slight effect on the uncertainties. In this case, it increases the uncertainties somewhat for the short simulation lengths. When enforcing a fixed stationary distribution, A_i are fixed as well and the uncertainties are 0.

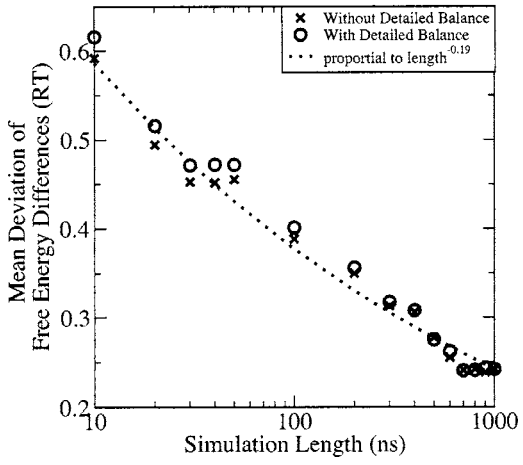

FIG. 6. Mean uncertainties of the free energy differences with respect to the starting state of the simulation for different simulation lengths. The uncertainties are shown for the ensembles of transition matrices and transition matrices with detailed balance.

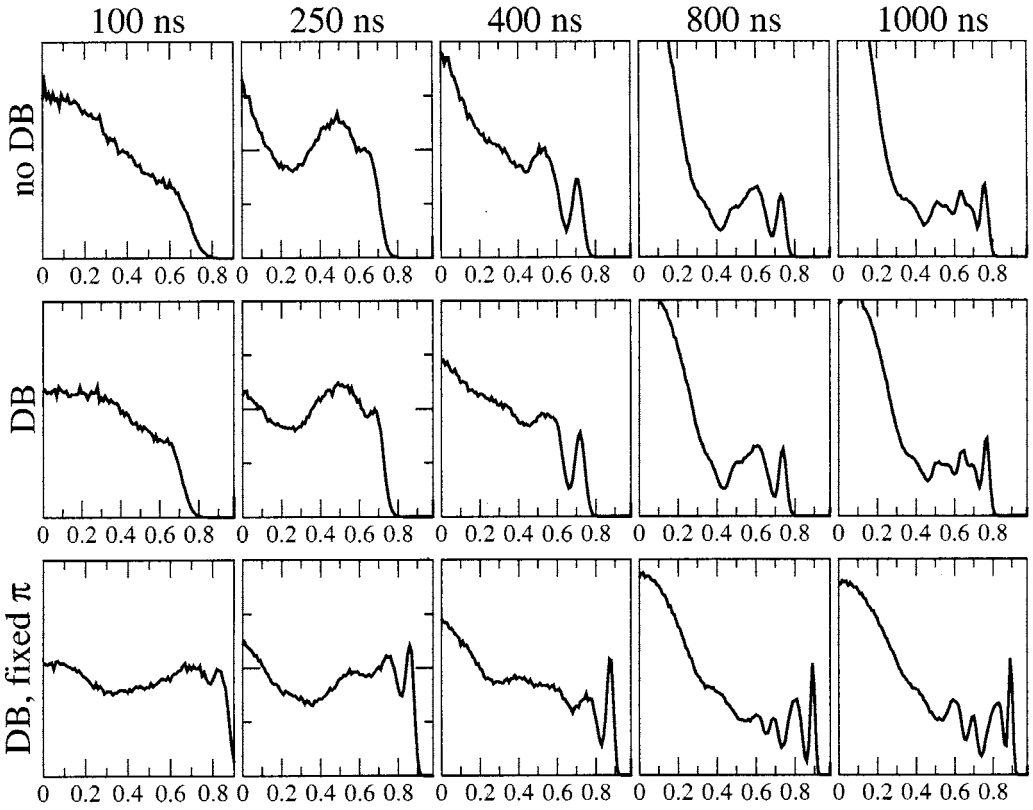

FIG. 7. Distributions of the eigenvalue spectrum of T for different simulation lengths. The distributions are shown for the ensembles of transition matrices [no detailed balance (DB)], transition matrices with DB, and fixed stationary distribution π.

Another interesting property of T is its spectrum, i.e., its eigenvalues λ_i with $i \in (1 \ldots m)$, which indicate the time scales of the transition processes in the system, τ_i^*, via Eq. (6). The first eigenvalue, which is always $\lambda_1 = 1$, is irrelevant in this respect as it only represents the fact that the system as a whole is never left ($\tau_1^* = \infty$). The next time scales $\tau_2^*, \tau_3^*, \ldots$ correspond to the time scales of the slowest and next-slowest transition processes. Due to the distribution of T, there is not a unique eigenvalue spectrum for a given observed transition count C, but rather a spectral distribution. With an increased number of observed transition counts, the uncertainties of individual λ_i will decrease, thus allowing for some of these λ_i to be distinguished from the rest of the spectral distribution. Figure 7 shows the spectral distribution for several simulation lengths. For simulation times up to 100 ns, the spectral distribution has no distinctive features. With increasing simulation time, some peaks at the large eigenvalue region start to form. From 400 ns on, the slowest transition process at $\lambda_2 \approx 0.75$ can be clearly distinguished and continues to narrow with yet increasing simulation time. At 1000 ns, the spectrum exhibits a lot of structure in the range $\lambda \geqslant 0.5$, but apart from λ_2 no peaks are clearly separated. This indicates that even for a small peptide, 1 μs simulation time is rather short when good convergence of the kinetics is expected. Introducing detailed balance has little effect on the large-eigenvalue (slow time) range of the spectrum, but significantly damps the eigenvalues close to 0. This is due to the fact that introducing detailed balance reduces the unphysical negative part of the spectrum. When a fixed stationary distribution is imposed, the change is rather drastic. Now, the spectrum also shows some structure at shorter simulation times. At 1000 ns, there are four clearly distinguishable peaks. Moreover, the spectrum is somewhat shifted towards the slower time scales.

V. CONCLUSION

Methods were introduced for approximating the probability density of Markov transition matrices induced by observed transition counts. Three algorithms are given, for sampling stochastic matrices, stochastic matrices that fulfill detail balance, and stochastic matrices that additionally have a predefined stationary distribution. The algorithms, based on Metropolis Monte Carlo, are easy to implement and exhibit good convergence properties.

Molecular dynamics in equilibrium always fulfills detailed balance. It has been shown that including detailed balance can significantly alter the distribution of transition matrices. In particular, it reduces the uncertainties in the off-diagonal transition probabilities, which may be important when computing kinetic properties, such as transition pathways or rates.

Imposing a constraint on the stationary distribution can affect the distribution of transition matrices dramatically. It was shown that such a constraint can significantly sharpen the spectral distribution of transition matrices, which indicates the time scales involved in the system's transition processes.

Constraints of this kind are of interest since sometimes experimental information is available that provides reliable

knowledge of particular properties of the system, such as stationary distributions or rates. The approach taken here represents a theoretically rigorous way to incorporate such experimental knowledge into computational models. Towards a more powerful approach, subsequent studies will focus on providing sampling methods that allow constraints to be incorporated in a general way.

A program to compute the sample distribution of transition matrices and derived observables can be freely downloaded from www.research.franknoe.de

ACKNOWLEDGMENTS

This work was funded by the DFG research center *Matheon*. I am grateful to Philipp Metzner and Christof Schütte for inspiring discussions.

APPENDIX A: MR121-GSGSW PEPTIDE SIMULATION SETUP

A 1 μs MD simulation of the MR121-GSGSW peptide in water at 293 K was performed with the GROMACS software package[18] and with the GROMOS96 force field.[19] Partial atomic charges for the dye MR121 were taken from Vaiana *et al.*[20] One peptide molecule in an extended conformation was solvated with water and placed in a periodic rhombic dodecahedron box large enough to contain the peptide molecule and $\approx$1.0 nm of solvent on all sides at a liquid density of 55.32 mol/l ($\approx$1 g/cm^3), producing 1155 water molecules. Water was modeled by the simple point charge (SPC) model.[21] The simulation was performed in the *NVT* ensemble using the isokinetic thermostat.[22] All bond lengths were fixed using the Lincs algorithm[23] and a time step of 2 fs for numerical integration was used. Periodic boundary conditions were applied to the simulation box and the long-range electrostatic interactions were treated with the particle mesh Ewald method[24] using a grid spacing of 0.12 nm combined with a fourth-order B-spline interpolation to compute the potential and forces in between grid points. The real space cutoff distance was set to 0.9 nm. The C-terminal end of the peptide was modeled as COO^- to reproduce a *p*H of about 7 as in the experimental conditions.[7] No counterions were added since the simulation box was already neutral (one positive charge on MR121 and one negative charge on the terminal COO^-). The coordinates were saved every 200 fs.

APPENDIX B: GENERATION OF MARKOV MODEL FROM MD TRAJECTORY

To distinguish all relevant conformations of the system, the peptide coordinates were fitted to the extended structure and then the state space was partitioned into small regions using a *k*-means clustering with $k=5000$. Using this definition, there is no microstate containing both folded and unfolded structures, i.e., the discretization is fine enough to characterize the folding process. A transition matrix, $\mathbf{T}^{\text{micro}}(\tau) \in \mathbb{R}^{5000\times5000}$, was computed from such discretized trajectory by simply counting transitions for a lag time of $\tau = 1$ ns. In order to define a Markov model with less states, it is useful to merge states that interconvert quickly, thus keeping states with high inter-state barriers separated. Here, the robust Perron cluster-cluster analysis (PCCA) method is employed,[7,25] which finds an appropriate kinetic clustering for a predefined number of metastable states. Here, the number of metastable states was determined such that their implied time scales were at least 2 ns, resulting in 34 states. The resulting state definition is Markovian at a lag time of $\tau=1$ ns. Thus, the trajectory was sampled every $\tau=1$ ns and provided a matrix of transition counts, $C \in \mathbb{R}^{34\times34}$, which was used as a base for the transition matrix sampling.

[1] A. Ostermann, R. Waschipky, F. G. Parak, and G. U. Nienhaus, Nature (London) **404**, 205 (2000).
[2] S. Fischer, B. Windshuegel, D. Horak, K. C. Holmes, and J. C. Smith, Proc. Natl. Acad. Sci. U.S.A. **102**, 6873 (2005).
[3] F. Noé, D. Krachtus, J. C. Smith, and S. Fischer, J. Chem. Theory Comput. **2**, 840 (2006).
[4] M. Jäger, Y. Zhang, J. Bieschke, H. Nguyen, M. Dendle, M. E. Bowman, J. Noel, M. Gruebele, and J. Kelly, Proc. Natl. Acad. Sci. U.S.A. **103**, 10648 (2006).
[5] A. Y. Kobitski, A. Nierth, M. Helm, A. Jäschke, and G. U. Nienhaus, Nucleic Acids Res. **35**, 2047 (2007).
[6] D. Wales, *Energy Landscapes* (Cambridge University Press, Cambridge, 2003).
[7] F. Noé, I. Horenko, C. Schütte, and J. C. Smith, J. Chem. Phys. **126**, 155102 (2007).
[8] J. D. Chodera, K. A. Dill, N. Singhal, V. S. Pande, W. C. Swope, and J. W. Pitera, J. Chem. Phys. **126**, 155101 (2007).
[9] H. Frauenfelder, S. G. Sligar, and P. G. Wolynes, Science **254**, 1598 (1991).
[10] N. G. van Kampen, *Stochastic Processes in Physics and Chemistry*, 4th ed. (Elsevier, Amsterdam, 2006).
[11] N. Singhal and V. S. Pande, J. Chem. Phys. **123**, 204909 (2005).
[12] N. S. Hinrichs and V. S. Pande, J. Chem. Phys. **126**, 244101 (2007).
[13] F. Noé, M. Oswald, G. Reinelt, S. Fischer, and J. C. Smith, Multiscale Model. Simul. **5**, 393 (2006).
[14] F. Noé, M. Oswald, and G. Reinelt, "Optimizing in graphs with expensive computation of edge weights," in *Operations Research Proceedings*, edited by J. Kalcsics and S. Nickel (Springer, New York, 2007), p. 435.
[15] L. Devroye, *Non-Uniform Random Variate Generation* (Springer, New York, 1986).
[16] J. Ahrens and U. Dieter, Commun. ACM **25**, 47 (1982).
[17] H. Neuweiler, M. Löllmann, S. Doose, and M. Sauer, J. Mol. Biol. **365**, 856 (2007).
[18] D. van der Spoel, E. Lindahl, B. Hess, G. Groenhof, A. E. Mark, and H. J. C. Berendsen, J. Comput. Chem. **26**, 1701 (2005).
[19] W. F. van Gunsteren and H. J. C. Berendsen, Angew. Chem., Int. Ed. Engl. **29**, 992 (1990).
[20] A. C. Vaiana, H. Neuweiler, A. Schulz, J. Wolfrum, M. Sauer, and J. C. Smith, J. Am. Chem. Soc. **125**, 14564 (2003).
[21] H. J. C. Berendsen, J. R. Grigera, and T. P. Straatsma, J. Phys. Chem. **91**, 6269 (1987).
[22] D. J. Evans and G. P. Morris, *Statistical Mechanics of Nonequilibrium Liquids* (Academic, London, 1990).
[23] B. Hess, H. Bekker, H. J. C. Berendsen, and J. G. E. M. Fraaije, J. Comput. Chem. **18**, 1463 (1997).
[24] T. Darden, D. York, and L. Pedersen, J. Chem. Phys. **89**, 10089 (1993).
[25] P. Deuflhard and M. Weber, ZIB Report, Report No. 03–09, 2003.